

A New Specimen of Microraptor (Theropoda: Dromaeosauridae) from the Lower Cretaceous of Western Liaoning, China

Authors: Pei, Rui, Li, Quanguo, Meng, Qingjin, Gao, Ke-Qin, and Norell, Mark A.

Source: American Museum Novitates, 2014(3821) : 1-28

Published By: American Museum of Natural History

URL: <https://doi.org/10.1206/3821.1>

BioOne Complete (complete.BioOne.org) is a full-text database of 200 subscribed and open-access titles in the biological, ecological, and environmental sciences published by nonprofit societies, associations, museums, institutions, and presses.

Your use of this PDF, the BioOne Complete website, and all posted and associated content indicates your acceptance of BioOne's Terms of Use, available at www.bioone.org/terms-of-use.

Usage of BioOne Complete content is strictly limited to personal, educational, and non - commercial use. Commercial inquiries or rights and permissions requests should be directed to the individual publisher as copyright holder.

BioOne sees sustainable scholarly publishing as an inherently collaborative enterprise connecting authors, nonprofit publishers, academic institutions, research libraries, and research funders in the common goal of maximizing access to critical research.

A new specimen of *Microraptor* (Theropoda: Dromaeosauridae) from the Lower Cretaceous of western Liaoning, China

RUI PEI¹, QUANGUO LI,² QINGJIN MENG,³ KE-QIN GAO,⁴
AND MARK A. NORELL⁵

ABSTRACT

Microraptor zhaoianus is known from several specimens collected in western Liaoning Province, China. However, several aspects of the morphology of *Microraptor* remain unknown or ambiguous due to poor preservation of the described specimens. A well-preserved new specimen of *Microraptor zhaoianus* is described in this study. This specimen preserves significant morphological details that are not present or are poorly preserved in the other *Microraptor* specimens including aspects of the skull, the rib cage, and the humerus. These new characters corroborate *Microraptor* as a member of the Dromaeosauridae as previously suggested and support the close relationship of troodontids and dromaeosaurids (Deinonychosauria). The morphology of the rib cage also suggests *Microraptor* and the early volant avialans very likely may have shared a similar mechanism to assist respiration.

INTRODUCTION

Microraptor is an important and interesting avianlike dinosaur from the Jehol Biota. It has received a lot of attention especially in regard to its possible volant activity, extensive plumage on

¹ Division of Paleontology, American Museum of Natural History.

² State Key Laboratory of Biogeology and Environmental Geology, China University of Geosciences, Beijing 100083, China.

³ Beijing Museum of Natural History, 126 Tianqiao South Street, Beijing 100050, China.

⁴ School of Earth and Space Sciences, Peking University, Beijing 100871, China.

⁵ Division of Paleontology, American Museum of Natural History.

its hind limbs, and feather coloration (Xu et al., 2000; Hwang et al., 2002; Xu et al., 2003; Hone et al., 2010; Li et al., 2012). The type species *Microraptor zhaoianus* was first reported by Xu et al. (2000) based on a single incomplete specimen (IVPP V12330) from Early Cretaceous rocks of the Jiufotang Formation, Liaoning Province, China, and was regarded as the most basal member of the Dromaeosauridae at that time. The so-called “four-winged dinosaur,” *Microraptor gui*, was reported as another nominal species from the same locality by Xu et al. (2003). The anatomy of *M. gui* is not significantly different from the type species *M. zhaoianus*, and thus, the species name has been considered a junior synonym of *M. zhaoianus* (Senter et al., 2004; Turner et al., 2012, but see O'Connor et al., 2011). A third species, *Microraptor hanqingi*, was reported from the same locality recently (Gong et al., 2012); however, the morphology is not distinguishable from other *Microraptor* specimens. We follow Turner et al. (2012) and consider these species names to be synonymous, and the term *Microraptor* is restricted to the type species *M. zhaoianus*.

The holotype of *Microraptor zhaoianus* was described in the original publication (Xu et al., 2000). However, it lacks many important parts of the skeleton, including most of the skull, almost all of the manus, the pectoral girdle, and dorsal vertebrae. Hwang et al. (2002) described and illustrated two additional *Microraptor* specimens (CAGS 20-7-004 and CAGS 20-8-001) from the same locality, giving detailed anatomical descriptions and figures of the lower jaws, teeth, and aspects of the postcranial skeleton. Xu (2002) redescribed the holotype and another *Microraptor* specimen (IVPP V13475) in his doctoral dissertation. The referred specimen IVPP V13475 is nearly complete, adding new information to the preorbital part of the skull. However, the skull of IVPP V13475 also lacks preservation of many anatomical details. Unfortunately, Xu's (2002) work has not been formally published and is not easily accessed. In both Xu et al.'s (2000) and Hwang et al.'s (2002) analyses, *Microraptor* was proposed to be the basalmost dromaeosaurid with several avialan and troodontid features; these are considered as primitive for Deinonychosauria. Later phylogenetic analyses with additional taxa and characters positioned *Microraptor* as a primitive, but not the basalmost dromaeosaurid since several more-basal dromaeosaurids were subsequently discovered (Turner et al., 2007a; Hu et al., 2009; Turner et al., 2012). However, all previous phylogenetic analyses involving *Microraptor* were derived from matrices with large amounts of missing data distributed through both the cranial and postcranial characters.

A new *Microraptor* specimen (BMNHC PH881) was recently acquired by Beijing Museum of Natural History from the same locality as the type specimen (Li et al., 2012). This specimen is very complete and includes a much better preserved skull compared with other *Microraptor* specimens (fig. 1). In addition to the skull and postcranial skeleton, BMNHC PH881 preserves an extensive body covering of feathers. Recently, this covering has been thoroughly described, and the feathers are shown to be black and iridescent in appearance like those of the extant Common Grackle *Quiscalus quiscula* (Li et al., 2012).

Currently the state of deinonychosaurian, and even paravian interrelationships, is in flux. Central to this problem are the relationships of several small paravian clades, most of which are known by fossils from the Jehol Group of northeastern China. We feel strongly that resolution of this part of the family tree is dependent on careful anatomical descriptions of these small taxa that will allow additional characters to be discovered, known characters to be scored, and levels of single-character variation to be adequately assessed. Consequently, we provide

only an update of character scorings for the new anatomical information based on the Turner et al. (2012) matrix. A more complete phylogenetic analysis of this clade cannot proceed until careful monographic descriptions of several taxa including *Jinfengopteryx*, *Anchiornis*, and *Xiaotingia* are completed. Here we develop a description of the BMNH PH881 specimen and provide appropriate codings for characters in the Turner et al. (2012) TWG 2012.1 matrix and discuss these characters in reference to other paravians.

MATERIAL

BMNH PH881 is a single slab with almost all the bones split on the same plane (fig. 1). Most of the bones are complete, unlike many of Jehol specimens, which are shattered, distorted, compressed, or broken longitudinally. Only some elements of the rib cage are missing (presumably falling off the slab when the slab was split), but their imprints are clearly present on the slab. The skeleton is nearly complete and fully articulated. Most of the skull is well preserved; however, the back of the skull and the braincase are crushed and provide little morphological information. Most of the postcranial skeleton is exposed, except portions of the pectoral girdle and the pelvic girdle. Some regions of the postcranium are not fully prepared, such as the presacral vertebral series and the left forelimb.

MORPHOLOGICAL DESCRIPTION

BMNH PH881 can be referred to *Microraptor zhaoianus* based on the combination of following diagnostic characters (Xu et al., 2000; Xu, 2002; Turner et al., 2012): teeth only serrated on posterior carinae; posterior teeth with a basal constriction between crown and root; middle caudal vertebrae about three to four times as long as anterior dorsals; manual phalanx III-3 less than one third as thick as manual phalanx II-2; accessory crest on femur at base of lesser trochanter; pedal phalanges III-1 and IV-1 much more robust than the other phalanges on the same digits; extremely long and bowed metatarsal V.

Feathers associated with the neck, forelimbs, hind limbs, and tail are preserved in BMNH PH881, and are particularly well preserved on the right forelimb, left hind limb, and tail as dark imprints. In contrast to *Anchiornis*, no preserved feathers are associated with the pedal digits (Xu et al., 2008). The feather morphology of BMNH PH881 was described in detail by Li et al. (2011). The asymmetrically vaned hind limb feathers are about 80% of the length of the asymmetrically vaned primary wing feathers, as reported in the referred specimen IVPP V13352 (Xu et al., 2003).

SKULL AND MANDIBLE

BMNH PH881 has a subtriangular skull that is very similar in profile to the basal avialan *Archaeopteryx* and several basal and juvenile troodontids (Elżanowski and Wellnhofer, 1996; Xu et al. 2002; Bever and Norell, 2009; Xu et al., 2008; Hu et al., 2009). Elements of the orbital region, such as the frontal, the jugal, and the postorbital are dislocated (fig. 2). Elements of the



FIGURE 1. *Microraptor zhaoianus*, BMNH PH881, view of entire mounted slab.

posterior part of the skull, including the parietal and the braincase, are too shattered to provide useful information.

PREMAXILLA: The right premaxilla is completely preserved and exposed in lateral view (figs. 2, 3). The anterior margin of the premaxilla forms a right angle where it meets the ventral margin. The nasal process forms the anterodorsal margin of the external naris. The prenasial portion of the premaxilla is mediolaterally thick, bearing pneumatic recesses on the lateral surface like in many dromaeosaurids, in contrast to the smooth surface of most troodontids. The internarial bar is slender, subcylindrical and slightly mediolaterally widened in cross section, like other dromaeosaurids and *Sinovenator* (Xu et al., 2002). The lateral surface of the main premaxillary body is rugose and shallow, with a length/depth ratio of 2.6, larger than that of derived dromaeosaurid taxa such as *Deinonychus* and *Velociraptor* (Ostrom, 1969; Barsbold and Osmólska, 1999), but similar to that of *Sinornithosaurus* and basal troodontids (Xu et al., 1999; Xu et al., 2002; Makovicky and Norell, 2004). A short subnasial process lies above the anterior tip of the maxilla, and excludes the maxilla from the floor of the external naris, as in other dromaeosaurids and *Sinovenator* (Xu et al., 2002; Norell and Makovicky, 2004). Like *Sinornithosaurus*, the subnasial process is much shorter compared to other dromaeosaurids in lateral view (Xu et al., 1999). The external naris is large and oval, and its long axis is inclined along an anteroventral-posterodorsal axis as in many basal deinonychosaurs, but different from more derived dromaeosaurid forms such as *Velociraptor* and *Tsaagan* and many troodontids, where the long axis of external naris is horizontally oriented (Barsbold and Osmólska, 1999; Norell et al., 2000; Norell et al., 2006).

The premaxilla bears four teeth, a primitive condition in nonavian theropods. All premaxillary teeth are lancet shaped and slightly recurved. The premaxillary teeth are more closely packed than those in many other dromaeosaurids, including small forms like *Sinornithosaurus* and NGMC 91 (Xu et al., 1999; Ji et al., 2001), but are more loosely packed than in most troodontids. The distance



FIGURE 2. The skull and the mandible of BMNH PH881 in lateral view.

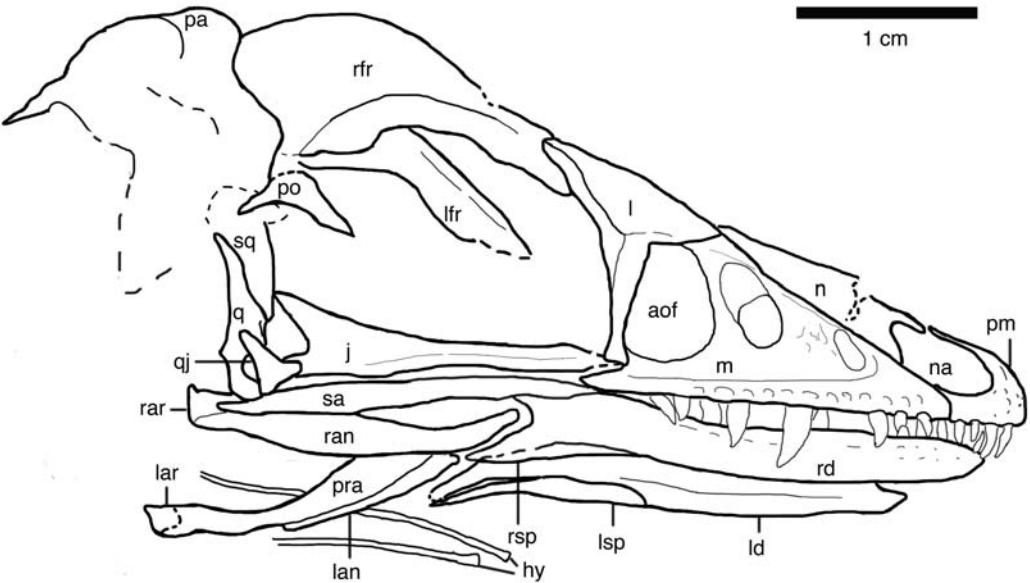


FIGURE 3. Interpretive drawing of the skull and the mandible of BMNH PH881.

between neighboring teeth is no more than one tooth wide. The second premaxillary tooth is the largest, while the 3rd and 4th teeth are relatively small as in other dromaeosaurids and *Epidexipteryx* (Zhang et al., 2008). Generally, the premaxillary teeth are smaller than the maxillary teeth, which is also a condition found in basal dromaeosaurids and most troodontids.

MAXILLA: The right maxilla is completely preserved and exposed in lateral view. The most apparent feature is the large triangular antorbital fossa (figs. 2, 3, and 4). The antorbital fossa has a well-developed ventral margin that is defined by a shelf on the ventral ramus of the maxilla, like in many dromaeosaurids and basal troodontids (Xu et al., 1999; Burnham et al., 2000; Xu et al., 2002), but the antorbital fossa is not as distinct as in oviraptorosaurs and therizinosaurids (Balanoff and Norell, 2012). A small and dorsoventrally elongate promaxillary fenestra is positioned at the anterior corner of the antorbital fossa, similar to the condition in *Anchiornis* (Hu et al., 2009). The distance between the promaxillary fenestra and the maxillary fenestra is relatively long, more than one fourth the length of the entire antorbital fossa, a condition found in basal dromaeosaurids such as *Sinornithosaurus* and *Bambiraptor* (Xu et al., 1999; Burnham et al., 2000). Like in *Sinornithosaurus*, the space between the promaxillary fenestra and the maxillary fenestra shows a wrinkled surface texture (Xu et al., 1999; Xu and Wu, 2001). A dorsoventrally elongate maxillary fenestra is located in the antorbital fossa, between the promaxillary fenestra and the antorbital fenestra (fig. 4). The maxillary fenestra is divided into two parts by a thin subhorizontal bar. A subtriangular fossa is above, and a square opening is below the bar, with the lower opening slightly larger than the upper fossa (figs. 3, 4). This feature of the maxillary fenestra appears novel, as it has not been reported in any other theropods. IVPP V13475 also has a similar maxillary fenestra in the same position, and it bears only a single opening (Xu, 2002). It is unclear whether this incongruence is due to preservation or individual variation. *Shanag* bears a similarly patterned maxillary fenestra, as a round opening within a shallow, caudally or caudodorsally open fossa (Turner et al., 2007b). The antorbital fenestra is pear shaped, with a longer ventral than dorsal margin, which differs from the condition in *Bambiraptor*, *Tsaagan*, and *Velociraptor*. In these taxa the antorbital fenestra is subtriangular with a longer dorsal margin (Barsbold and Osmólska, 1999; Burnham et al., 2000; Norell et al., 2006). The anteroposterior diameter of the antorbital fenestra is less than half the length of the antorbital fossa, as in *Sinornithosaurus* (Xu et al., 1999). The area of the antorbital fenestra is proportionally smaller than in other dromaeosaurids, such as *Bambiraptor*, *Velociraptor*, and *Dromaeosaurus* (Colbert and Russell, 1969; Barsbold and Osmólska, 1999; Burnham et al., 2000). The antorbital fenestra is separated from the maxillary fenestra by a slender interfenestral bar, similar to the troodontid condition and *Sinornithosaurus* (Xu et al., 1999; Makovicky and Norell, 2004). The interfenestral bar is anteroventrally inclined, and the lower half of the bar is anteroposteriorly expanded like in many deinonychosaurians, such as *Velociraptor*, *Tsaagan*, and *Sinovenator* (Barsbold and Osmólska, 1999; Xu et al., 2002; Norell et al., 2006). The ventral ramus of the maxilla forms the ventral border of the antorbital fossa. It extends from the blunt anterior process and tapers posteriorly toward its contact with the lacrimal and the jugal. Several neurovascular foramina are elongate and are arranged in a linear fashion on the lateral surface along the maxillary ventral rim (figs. 2, 3).

Thirteen tooth positions are present on the right maxilla as reported in the holotype (Xu et al., 2000). All the teeth are loosely packed, and are more evenly spaced compared to those

of *Sinovenator*, in which the maxillary teeth are more closely packed at the anterior part of the tooth row (Xu et al., 2002). The maxillary teeth are recurved and laterally compressed, with a slightly convex lateral surface. The height of each tooth crown is about three times its width, similar to most dromaeosaurids but thicker than in *Sinornithosaurus* (Xu et al., 1999). No apparent constrictions are observed between the crown and the root, except on the last exposed maxillary tooth. Teeth in the middle of the maxillary tooth row are larger than those of anterior and posterior part of the tooth row (figs. 2, 3), as is typical in many other dromaeosaurids and some basal troodontids (Colbert and Russell, 1969; Xu et al., 1999; Xu et al., 2002; Norell and Makovicky, 2004). The largest maxillary tooth is about three times the height of the first tooth and twice as tall as the last; similar to *Sinornithosaurus*, the largest maxillary tooth is more than twice the height of the first and the last maxillary teeth (Xu et al., 1999). Teeth in the middle of the maxillary tooth row bear serrations only on their posterior carinae like *Sinornithosaurus* and some troodontids (Xu et al., 1999; Xu et al., 2002), but different from most other dromaeosaurids, in which the teeth are serrated both anteriorly and posteriorly (Norell and Makovicky, 2004). The serrations are fine and simple as seen in the referred specimen CGAS 20-7-004 (Hwang et al., 2002). The serration density of the largest maxillary tooth is 11 per mm, in contrast to 8 per mm of CGAS 20-7-004 (Hwang et al., 2002).

NASAL: The right nasal is exposed, yet compressed and in quasilateral view. Its anterior portion is damaged due to a fracture on the slab (figs. 2, 3). The left nasal is buried beneath the maxilla and is partially exposed through the maxillary fenestra and the antorbital fenestra. The dorsal surface of the nasal is depressed slightly, but not as much as in other dromaeosaurids like *Sinornithosaurus*, *Velociraptor*, and *Tsaagan* (Barsbold and Osmólska, 1999; Xu et al., 1999; Norell et al., 2006). The nasal's ventral surface is rugose, as observed through the antorbital fenestra, but the entire pattern is not clear.

FRONTAL: The right frontal is slightly dorsally dislocated, and is damaged where it meets the parietal and the postorbital. The left frontal is preserved beneath the right frontal and the anterior portion is exposed in medial view through the orbit (figs. 2, 3). The frontal contacts the nasals anteriorly and the lacrimal anterolaterally. A groove on the frontal beneath the right lacrimal indicates the position where the frontal received the lacrimal like in other deinonychosaurs (Currie, 1995; Norell et al., 2006; Turner et al., 2011). The frontal is vaulted above the orbit. A sharp supra-orbital rim is developed along the orbital margin of the frontal, bordering the orbit posterodorsally. The frontal turns abruptly inward below the supraorbital rim toward the midline, forming the upper portion of the lateral wall of the braincase. A groove is present ventral to the supraorbital rim, but is limited in the portion right above the orbit like in *Anchiornis* (Hu et al., 2009).

LACRIMAL: The right lacrimal is completely preserved in lateral view (figs. 2, 3, and 4). It is T-shaped as exposed, similar to those of dromaeosaurids and troodontids (Makovicky and Norell, 2004; Norell and Makovicky, 2004). The anterior and posterior processes are subequal in length like in many dromaeosaurids (Norell and Makovicky, 2004; Turner et al., 2012). This condition is in contrast to most derived troodontids, in which the anterior processes are much longer than the posterior processes (Makovicky and Norell, 2004). The lacrimal body is formed by the triple junction among the anterior, posterior, and ventral processes and is primarily exposed on the dorsal roof of the skull. The main body of the lacrimal is triangular in dorsal

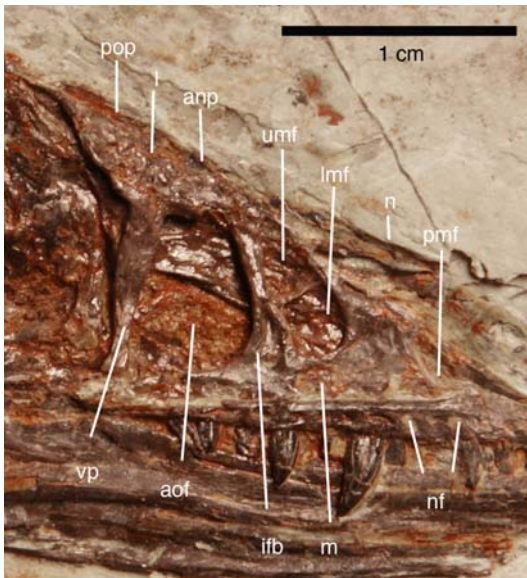


FIGURE 4. The maxilla and the lacrimal of BMNH PH881 in lateral view.

edge of the posterior process also laterally expands to form a thick anterodorsal margin of the orbit. The ventral edge of the posterior process turns ventrally at the lateral apex of the lacrimal to form a vertical ridge along the lateral/posterolateral side of the ventral process. The ventral process separates the antorbital fossa from the orbit. Ventrally, it tapers slightly to form a tight articulation with the anterior end of the jugal. An opening of the lacrimonasal duct is present anterior to the orbit and on the posterior surface of the ventral process.

JUGAL: The right jugal is slightly dislocated from its original position. It is exposed in lateral view, and the anterior end of the suborbital process is damaged (figs. 2, 3). The jugal is tripartite and platelike, as in other dromaeosaurids, such as *Tsaagan* and *Velociraptor* (Barsbold and Osmólska, 1999; Norell et al., 2006). The suborbital process is long and slender and tapers anteriorly. It contacts the ventral process of the lacrimal at the anteroventral corner of the orbit like in other dromaeosaurids (Norell and Makovicky, 2004). The lateral surface of the suborbital process is rugose and anterior-posteriorly grooved, like in *Sinovenator* (Xu et al., 2002). The postorbital process is short and tapers posterodorsally, and it forms the lower portion of the postorbital bar. A short quadratojugal process contacts the quadratojugal posteriorly and forms the ventral margin of the lower temporal fenestra.

POSTORBITAL: Only a partial right postorbital is preserved in lateral view, and it is dislocated from its original position. The frontal process is missing and the jugal process is damaged (figs. 2, 3). The jugal process does not contact the jugal due to preservation. As in other dromaeosaurids (Norell and Makovicky, 2004), it probably tapered ventrally or anteroventrally in its original position, and contacted the postorbital process of the jugal with a suture that is inclined anteroventrally. The squamosal process is slender and tapers posteriorly.

QUADRATOJUGAL: The right quadratojugal is exposed in lateral view (figs. 2, 3). It is slightly eroded and dislocated. The quadratojugal is an inverted T-shape as is typical of dromaeosaurids

view, with a prominent lateral expansion anterodorsal to the orbit. The lateral apex (the lateralmost projected part of the lateral expansion) is on the midline of the lacrimal, in contrast to the condition in *Sinornithosaurus*, *Bambiraptor*, and *Tsaagan* where the lateral apex is more posteriorly positioned (Xu et al., 1999; Burnham et al., 2000; Norell et al., 2006). The anterior process tapers anteriorly, with a straight ventral border, forming the entire dorsal margin of the antorbital fenestra. This condition is different from that in other dromaeosaurids where the anterior process of the lacrimal forms only part of the dorsal margin of the antorbital fenestra (figs. 3, 4). The posterior process, which begins posterior to the lateral apex, extends posterodorsally, and its ventral edge is slightly sinusoidal. The ventral

(Norell and Makovicky, 2004). Anteriorly, a short anterior process overlaps the quadratojugal process of the jugal laterally. Posteriorly, the quadratojugal forms the lateral margin of a large quadrate foramen, which is present in many dromaeosaurids (Barsbold and Osmólska, 1999; Norell et al., 2006). The posterior process of the quadratojugal contacts the articular ramus of the quadrate, and the dorsal process probably contacted the anterior phalange of the quadrate if in its original position.

QUADRATE: The right quadrate is preserved in lateral view, and its anterior margin is damaged (figs. 2, 3). BMNH PH881 is similar to other dromaeosaurids in having a distinct squamosal ramus and a distinct articular ramus of the quadrate. The squamosal ramus sutures to the descending process of the squamosal. The articular ramus contacts the posterior process of the quadratojugal, and forms the medial margin of the quadrate foramen. The ventral end of the articular ramus appears transversely expanded and has a bicondylar articulation with the mandible. A faint ridge at the anterior margin of the quadrate likely represents the anterior flange.

SQUAMOSAL: Only the descending process of the right squamosal is preserved. It is anteroposteriorly wider than the squamosal ramus of the quadrate in lateral view (figs. 2, 3).

The back of the skull and the braincase are shattered and dislocated, preserving little information. A sharp transverse ridge is present posterodorsally on the skull, which probably represents a posterior parietal crest.

DENTARY: The right dentary is exposed in lateral view and the left dentary is exposed in medial view (figs. 2, 3). The dentary is long and slender, with a length/depth ratio of approximately 10. The dorsal margin of the anterior tip slopes anteroventrally as in most dromaeosaurids and ornithomimosaurs as well as some troodontids, especially juveniles as in *Byronosaurus* (Bever and Norell, 2009). The anteriormost part of the lateral surface is rugose. The dorsal and ventral margins of the dentary are nearly parallel along most of the length of the bone, as is typical of dromaeosaurids and some basal avialans (Norell and Makovicky, 2004). The dentary tooth row is slightly inset. Two rows of neurovascular foramina penetrate the lateral surface of the dentary ventral to the tooth row, like in other dromaeosaurids (Currie, 1995; Xu et al., 1999). The ventral margin of the dentary is slightly convex as is typical of dromaeosaurids, such as *Sinornithosaurus* and *Velociraptor* (Barsbold and Osmólska, 1999; Xu et al., 1999). The den-

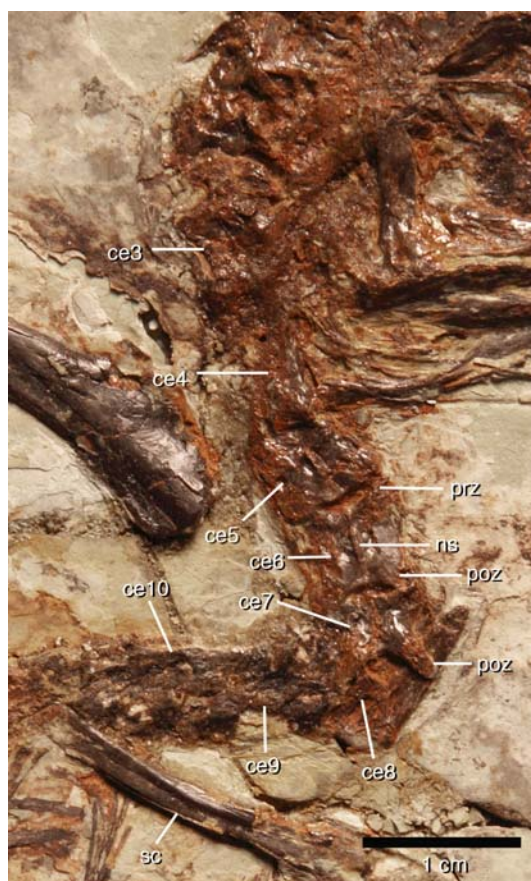


FIGURE 5. Cervical vertebrae and the right scapula of BMNH PH881.

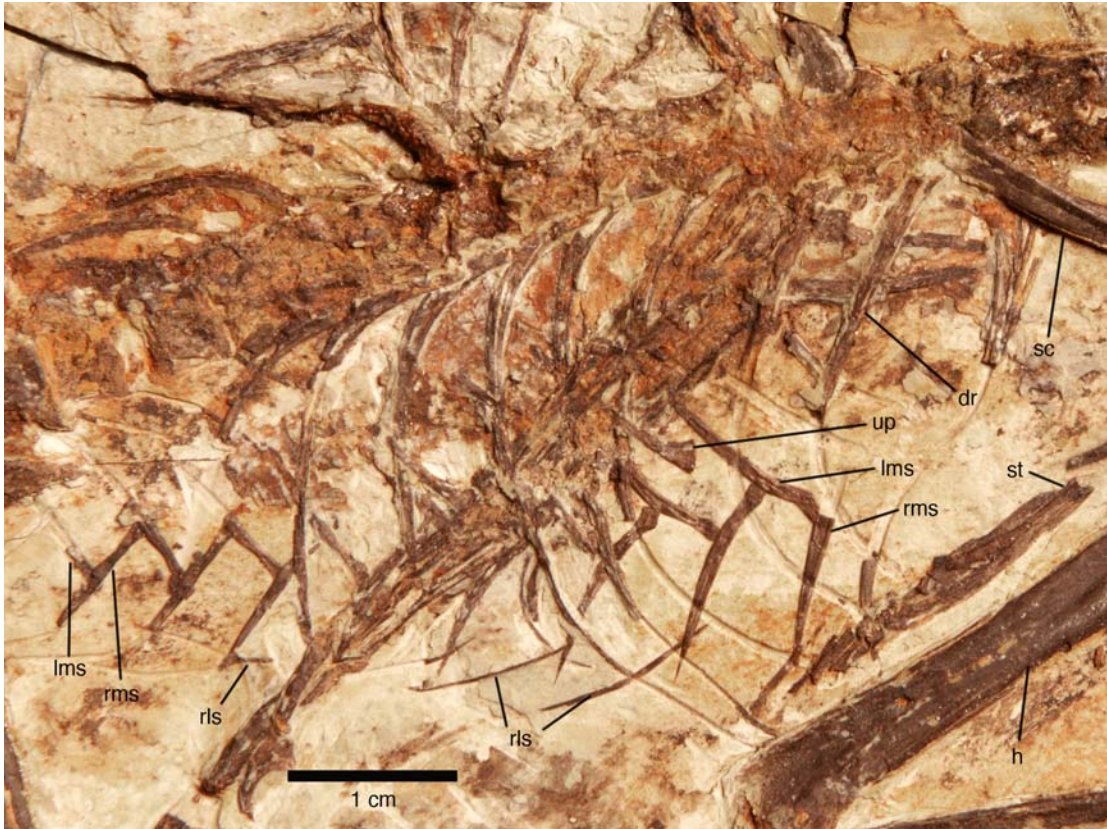


FIGURE 6. The rib cage of BMNHC PH881.

tary is deeper posteriorly than anteriorly, with a bifurcated posterior end like in *Sinornithosaurus* and NGMC 91 (Xu et al., 1999; Ji et al., 2001). The posterodorsal branch of the bifurcated posterior end forms part of the anterodorsal margin of a large and anterior-posteriorly elongate external mandibular fenestra (fig. 3). The posteroventral branch of the dentary is longer than the posterodorsal branch, and contacts the subfenestral process of the angular ventrally. On the medial surface, a deep Meckelian groove is present along the dentary bone (figs. 2, 3).

Six teeth are exposed on the right dentary and undoubtedly more are buried in the slab or hidden beneath the maxilla. The shape of the dentary teeth is similar to the premaxillary and the maxillary teeth. The anterior dentary teeth are more closely packed than the maxillary teeth. The exposed dentary teeth do not bear serrations on either carina. The size of each dentary tooth is subequal to, or slightly smaller than, the corresponding premaxillary and maxillary tooth.

SPLENIAL: The splenial is exposed on both mandibles (figs. 2, 3). The right splenial wraps the posteroventral branch of the right dentary ventrally. It has a subtriangular lateral exposure posteroventral to the dentary as observed in dromaeosaurids and some troodontids (Makovicky and Norell, 2004; Norell and Makovicky, 2004). The left splenial is exposed on the left mandible medially. It is slender and wraps the left dentary posteroventrally.

ANGULAR: The right angular is exposed in lateral view (figs. 2, 3). A slender anterior process forms the ventral margin of the external mandibular fenestra. This process is slightly

upturned. The angular also forms the ventral margin of the mandible posterior to the dentary and the splenial. The left angular is exposed on the left mandible medially. It is slender, and sutures with the dentary anteroventrally and the prearticular posterodorsally.

SURANGULAR: The right surangular is exposed in lateral view (figs. 2, 3). It is elongate and forms the entire dorsal margin of the longitudinally elongate external mandibular fenestra. The surangular is laterally everted at the dorsal margin of the mandible.

PREARTICULAR: The prearticular is exposed on the left mandible medially (figs. 2, 3). It is a curved bone that forms much of the medial surface of the posterior mandible as in other dromaeosaurids and *Archaeopteryx* (Elzanski, 2001; Norell et al., 2006). Ventrally it sutures to the angular, and posteriorly it meets the articular at the retroarticular process.

ARTICULAR: Both articulators are exposed at the posterior end of the mandibles (figs. 2, 3). The articular forms most of the short retroarticular process and the quadrate articular surface. A vertical columnar process is present posterior to the glenoid as is typical in dromaeosaurid dinosaurs (Currie, 1995).

HYOID: Both hyoids are preserved in BMNHC PH881. They are positioned at the bottom of the skull and exposed ventral to the mandible in this specimen (figs. 2, 3). The hyoid is a slender rodlike bone, as seen in *Sinornithosaurus* (Xu et al., 1999). The proximal portion of the hyoid is curved dorsally. The distal portion of hyoid lies parallel to the mandible and is slightly sinusoidal. The distal end of the hyoid is slightly expanded and mediolaterally compressed. The hyoid is more than one third of the length of the mandible.

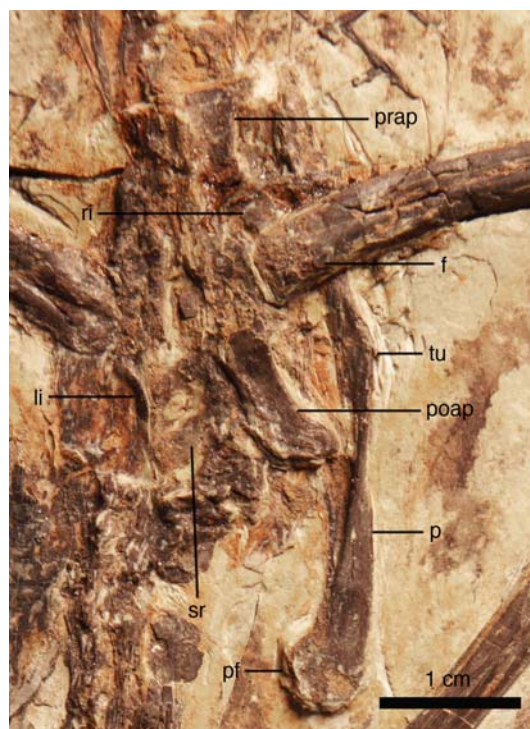


FIGURE 7. The pelvic region of BMNHC PH881 in dorsal view.

POSTCRANIUM

Several new features revealed in the postcranium of BMNHC PH881 include character information on the cervical vertebrae, the rib cage, and the humerus. Most aspects of the postcranial skeleton that can be directly compared are identical to the specimens described by Hwang et al. (2002) and Xu (2002), such as the elements of the pelvic and pectoral girdles, the limb bones, and details of the vertebral column.

VERTEBRAE: Only two posterior cervical vertebrae have been previously described (Hwang et al., 2002; Xu, 2002) for *Microraptor zhaoianus*. All of the cervical vertebrae are tightly articulated in the specimen (BMNHC PH881) described here (fig. 5). As reported in the referred speci-

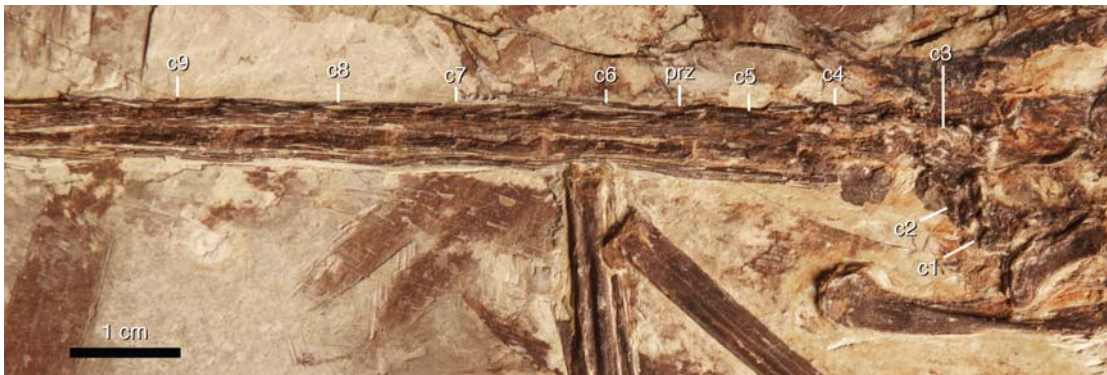


FIGURE 8. Proximal caudal vertebrae of BMNHC PH881.

men IVPP V13475 (Xu, 2002), 10 cervical vertebrae are preserved in BMNHC PH881. The cervical vertebrae are exposed in dorsal view, so detailed anatomical information is limited to this perspective (fig. 5). The neural arches of the 3th and 4th cervicals are damaged, and they appear narrower than the succeeding ones. The 5th to the 7th cervicals have a dorsally X-shaped neural arch with short neural spines as typical of deinonychosaurs (Norell et al., 2001). The prezygapophyses of the 5th through the 7th cervicals are shorter than the postzygapophyses. The prezygapophyses project anterolaterally on the 5th and 6th cervicals, but are more laterally expressed on the 7th cervical (fig. 5). The postzygapophyses are posterolaterally directed.

The trunk region of the vertebral column is primarily exposed in lateral view, although it is poorly preserved especially with the anterior and middle dorsal vertebrae (fig. 6). The exact number of dorsal vertebrae is difficult to determine; however, we estimate that 13–14 dorsals are present, whereas 13 dorsal vertebrae are estimated in CAGS 20-8-001 (Hwang et al., 2002). The posterior dorsals are square in lateral view. The posterior dorsal vertebrae are slightly shorter than the midcervical vertebrae.

The sacrum is visible in dorsal view although the anterior sacra are obscured by the ilium (fig. 7). The number of sacral vertebrae is estimated at five or six as in other specimens of *Microaptor* (Hwang et al., 2002). The sacral vertebrae are connected to the pelvic girdle by elongate sacral ribs, which expand laterally.

The tail of BMNHC PH881 is completely preserved. It is characterized by the extremely long extensions of the prezygapophyses and chevrons (fig. 8), as seen in other dromaeosaurids (Ostrom, 1969; Norell and Makovicky, 2004). The exact number of the caudal vertebrae cannot be determined because many of the vertebrae in the midportion of the tail are obscured by overlying prezygapophyses and chevrons. Nevertheless, we estimate 25–26 caudals were present as in *Microaptor* specimens described by Hwang et al. (2002) whereas 24–25 caudals were estimated in the holotype (Xu, 2002). The anterior caudals are short. Some square platelike elements that are scattered around the proximal portion of the tail probably represent the disassociated transverse processes of the anterior caudal vertebrae. The prezygapophyses on the anterior caudal vertebrae are approximately three times as long as the short postzygapophyses and overlap about one third of the preceding vertebra. The transition from the short anterior caudal vertebrae to the elongate middle caudal vertebrae begins at the sixth caudal as described

in CAGS 20-8-001 (Hwang et al., 2002). The rodlike extensions of the prezygapophyses and chevrons begin on midcaudal vertebrae, and they reach the third caudal vertebra anteriorly. The longest middle caudal vertebra is more than three times the length of the anteriormost caudal vertebrae as in CAGS 20-7-004 (Hwang et al., 2002). The caudal vertebrae diminish in length and height further posteriorly.

RIB CAGE: At least 10 dorsal ribs are preserved on the right side (fig. 6). A deep groove is present along the rib shaft anteriorly as noted in the holotype (Xu, 2002). The middle dorsal ribs are longer than the posterior ones, which is different from the avialan condition where the posterior dorsal ribs are longer.

Uncinate processes and gastralria were reported in the holotype IVPP V12230, referred specimens IVPP V13352, CAGS 20-7-004, and CAGS 20-8-001 (Xu et al., 2000; Hwang et al., 2002; Xu et al., 2003). They are much better preserved in this specimen as they remain mostly in life articulation (fig. 6). Three uncinate processes are preserved on the right side of the rib cage (fig. 6), whereas seven pairs of uncinate processes are reported in the referred specimen IVPP V13352 (Xu et al., 2003). The uncinate processes are anteroventral-posterodorsally oriented. They have bell-shaped heads and taper distally. Uncinate processes are also known for a variety of dromaeosaurids and oviraptorosaurs such as *Velociraptor*, NGMC 91, *Oviraptor*, and *Citipati* (Clark et al., 1999; Norell and Makovicky, 1999; Ji et al., 2001; Claessens, 2004). The morphology of uncinate processes is similar in these taxa, except for the geometry. The heads of the uncinate processes are preserved between dorsal ribs in BMNH PH881, but they are attached to the caudal edge of dorsal ribs in IVPP V13352, and this difference is likely caused by a preservational artifact. The uncinate process can span across three dorsal ribs if in its original position, as reported in the referred specimen IVPP V13352, as well as other maniraptorans, such as *Velociraptor* and *Confuciusornis* (Norell and Makovicky, 1999; Chiappe et al., 1999). An estimated six dorsal ribs are associated with uncinate processes in BMNH PH881.

The gastralria are articulated to the distal end of the dorsal ribs. Both lateral and medial segments of the gastralria are preserved, while only single gastralria segments were reported in CAGS 20-8-001 (Hwang et al., 2002). Both sides of the medial segments and the right set of the lateral segments are preserved underneath the right ribs, and most of the gastralria are preserved in articulation with each other (fig. 6). The medial segments are slightly bowed, with enlarged heads, and taper posterolaterally. The head of the medial segment is square in dorsal view, and it attaches to the shaft of the corresponding medial segment of the other side. The medial segments of both sides imbricate with each other to form a basketlike structure, a condition that is typical of many

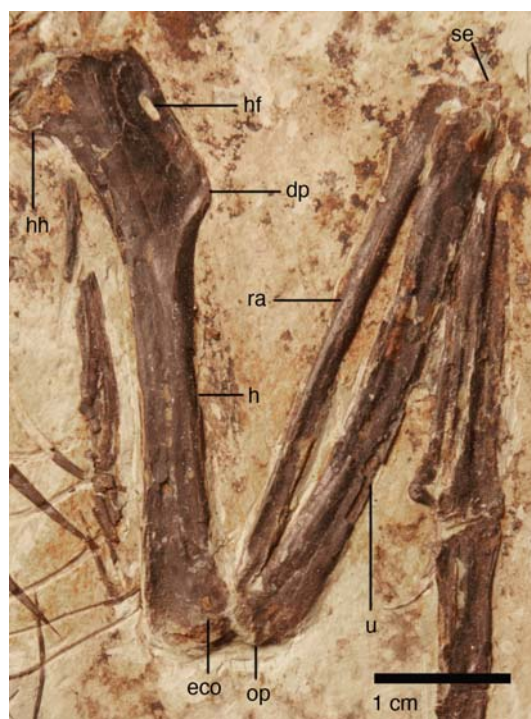


FIGURE 9. The right forelimb of BMNH PH881.

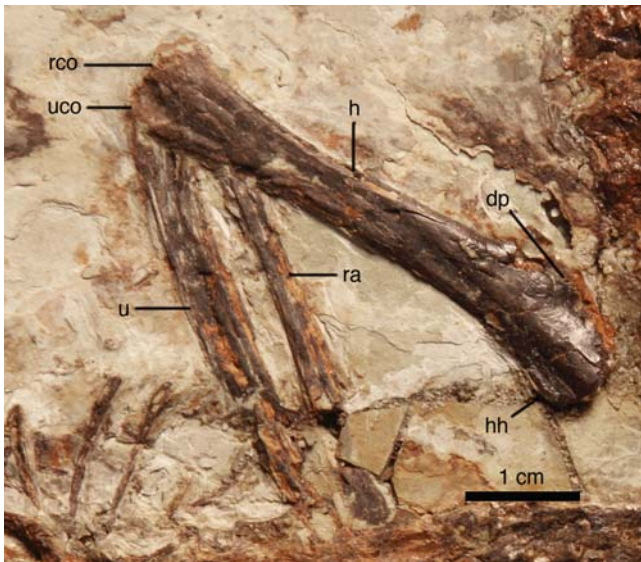


FIGURE 10. The left forelimb of BMNH PH881.

theropod dinosaurs (Claessens, 2004). The tapering lateral end of the medial segment is closely positioned with the gastralia lateral segment. The anterior medial segments are longer and strap-like, in contrast to the shorter and rodlike posterior medial segments. The lateral segments are subequal in length to the medial segments, which is different from the condition observed in *Sinornithoides*, *Velociraptor*, and *Linheraptor*, where the lateral segments are apparently longer (Russell and Dong, 1993; Norell and Makovicky, 1997; Xu et al., 2010). The lateral segments are bowed, and both ends of each segment are pointed.

PECTORAL GIRDLE: Only a partial right scapula is observable. The distal end and the acromion region of the right scapular are damaged. The scapular blade is long and straplike, slightly curved dorsally. A long bony element ventral to the anterior dorsal ribs may represent the compressed sternal plates. However, the shape of the sternum is ambiguous. Sternal ribs are observed in articulation with the sternal plate on the right side.

FORELIMB: Both humeri are well preserved in BMNH PH881. The right humerus is exposed in posterolateral view (fig. 9). The left humerus is exposed posterolaterally, with the humeral head and the deltopectoral crest damaged (fig. 10). The morphology of the left humerus is the mirror image of the right element. The humeral shaft is only slightly thicker than the ulna. As noted by Xu et al. (2000) and Hwang et al. (2002), the proximal end of the humerus bears a prominent humeral head and well-developed internal tuberosity as in other dromaeosaurids. The deltopectoral crest extends less than one third the length of the humeral shaft. The deltopectoral crest is square in lateral view. A distinct ovoid foramen is developed on the lateral side of the crest (fig. 9), which was not reported in previous works, but a similar structure exists in the referred specimen CAGS 20-8-001 and IVPP V13352 (Hwang et al., 2002; Xu et al., 2003). Such a structure is also present in some basal avialans, such as *Confuciusornis* (Chiappe et al., 1999). The distal end of the deltopectoral crest is thick, extending downward to join the humeral shaft anterolaterally. At the distal extremity, the radial condyle of the humerus is large and rounded. An ectepicondyle is attached to the radial condyle anterolaterally. A wide intercondylar groove separates the radial condyle from the ulnar condyle on the distal end.

Both the right radius and ulna are well exposed (fig. 9). The left radius and ulna are damaged by a crack on the slab, and both their ends are obscured by the overlying left humerus and dorsal vertebra respectively. The right ulna is about 95% of the humeral length and is only slightly thinner at midshaft than that of the humerus. The shaft of the ulna slightly bends inward as in other maniraptorans (Gauthier, 1986). The olecranon process is moderately developed, but the trian-

gular shape typical of coelurosaurs, mentioned by Xu (2002) and Hwang et al. (2002), is not observed due to the damage on the proximal tip of the process. The distal end of the ulna is rounded. The radius is straight and much more slender than the ulna. The radial shaft is about half the thickness of the ulna. The distal end of the radius is expanded. The morphology of the left radius and ulna are identical to the right elements (fig. 10).

Only one carpal is observed on the right side of the specimen. Since the triangular carpal is attached to the proximal end of the metacarpals, it is interpreted as the semilunate (figs. 9, 11).

The manus is elongate like in most deinonychosaurians (Ostrom, 1969; Makovicky and Norell, 2004; Norell and Makovicky, 2004). The left manual elements are mostly obscured by the rib cage, except the distal phalanges. The right manus is well exposed in lateral view (fig. 11), while metacarpal I is largely obscured by metacarpal II. Metacarpals II and III are subequal in length. Metacarpal II is straight and remains the same thickness throughout its length, and the distal end is ginglymoid. Metacarpal III is more slender than metacarpal II.

Manual phalanx I-1 is probably subequal in thickness to metacarpal III. The total length of manual phalanx I-1 and metacarpal I is less than the length of metacarpal II, as also observed in IVPP V13352 and *Sinornithosaurus* (Xu et al., 1999; Xu et al., 2003). Manual digit II is the longest and the most robust digit, bearing two elongate and robust phalanges. Digit II is probably as thick as metacarpal II. Manual phalanx II-1 is almost three times as thick as phalanx III-1 (fig. 11), as a unique character observed only in *Microraptor* (Xu et al., 2000). Phalanx II-2 is approximately the same length of phalanx II-1, and the shaft becomes thinner distally. The ungual phalanx II-3 has large flexor tubercles and is strongly recurved. Phalanges of digit III are much thinner in diameter than phalanges of digit II. Manual phalanx III-1 is slender and straight. Manual phalanx III-2 is extremely reduced, about one fifth the length of phalanx III-1, and the reduced phalanx III-2 is also seen in a wide range of dromaeosaurids (Norell and Makovicky, 2004). Manual phalanx III-3 is bowed and slightly shorter than phalanx III-1. The ungual phalanx III-4 is much smaller and less curved than ungual phalanges I-2 and II-3.

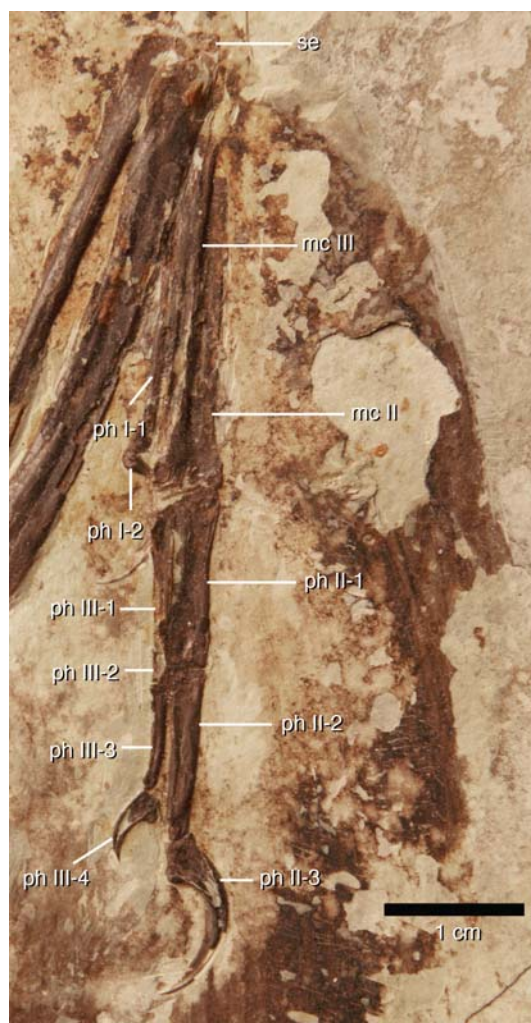


FIGURE 11. The right manus of BMNH PH881.



FIGURE 12. The right hind limb of BMNH PH881.

PELVIC GIRDLE: In BMNH PH881, both ilia are compressed and exposed in lateral view (fig. 7). The right ilium is mostly well preserved, except the anterior end of the preacetabular process, which is damaged. The ilium is dorsoventrally shallow and slender, about 57% of the femoral length, which is slightly proportionally longer than that in the referred specimen CAGS 20-8-001 (54%; Hwang et al., 2002). The preacetabular projects anteriorly and the anterior end hooks anteroventrally, as noted in CAGS 20-8-001 (Hwang et al., 2002). The antiliac shelf is short and no distinct cuppedicus fossa is present, which is a condition similar to *Saurornithosaurus* but different from larger derived dromaeosaurid taxa, such as *Velociraptor* (Norell and Makovicky, 1997; Xu et al., 1999). The pubic peduncle is triangular in outline, and it is much larger than the ischial peduncle, which is the primitive condition seen in deinonychosaurs, such as *Saurornithosaurus*, *Bambiraptor*, *Sinovenator*, and *Mahakala* (Xu et al., 1999; Burnham et al., 2000; Xu et al., 2002; Turner et al., 2011). The ventral margin of the pubic peduncle slopes posteroventrally. On the lateral surface of the ilium, a concavity is developed dorsal to the acetabulum. The postacetabular process tapers posteriorly to a rounded end and hooks posteroventrally. The posteroventral tip of the postacetabular process

descends further ventrally than both peduncles, as observed by Hwang et al. (2002). The lateral surface of the postacetabular process is concave.

The paired pubes are preserved in posterolateral view, with the right pubis partially overlapping the left (fig. 7). The morphology of the proximal end is unknown due to poor preservation. The proximal half of the pubic shaft is anteroposteriorly flat. The lateral edge of the midshaft expands into a small tubercle, which is similar to that in *Sinornithosaurus*, NGMC 91, and *Sinovenator* (Xu et al., 1999; Ji et al., 2001; Xu et al., 2002). This structure may represent the curved pubis as observed in IVPP V13352 (Xu et al., 2003). The distal half of the pubic apron curves posteriorly. The pubic foot is mediolaterally flattened and bears a round expansion posteroventrally.

Neither of the ischia is visible.

HIND LIMB: Both femora are well preserved. The right femur is exposed posterolaterally (fig. 12). The proximalmost part of the right femur is eroded; thus, information concerning the femoral head is missing. The shaft of the femur is slightly bowed as is typical for paravians (Norell and Makovicky, 2004; Turner et al., 2012). Distally, the lateral condyle and medial condyle are subequal in size. A well-developed popliteal groove is developed between the condyles posteriorly. The lateral side of the lateral condyle is convex and forms a low ridge in posterior view. The left femur is laterally exposed (fig. 13). The broad greater trochanter of the femur is separated from the cylindrical lesser trochanter by a distinct groove. The proximal margin of the lesser trochanter is slightly below that of the greater trochanter. At the base of the lesser trochanter, a small ridge represents the accessory crest, as noted in the holotype IVPP V12330 and CAGS 20-8-001 (Xu et al., 2000; Hwang et al., 2002). The posterolateral surface of the femur distal to the greater trochanter is rugose as in referred specimens (Hwang et al., 2002), possibly representing the posterior trochanter. The lateral condyle is generally rounded in lateral view. It is posteroventrally projected, without a prominent expansion.

The tibiotarsus and fibula on either side are well preserved and exposed in posterior view (figs. 12, 13). The tibia is long and straight, approximately 136% of the femoral length. Proximally, the tibia is only slightly expanded, not as much as in basal troodontids, such as *Sinovenator* and *Anchiornis* (Xu et al., 2002; Xu et al., 2008; Hu et al., 2009). The cnemial crest



FIGURE 13. The left hind limb of BMNH PH881.

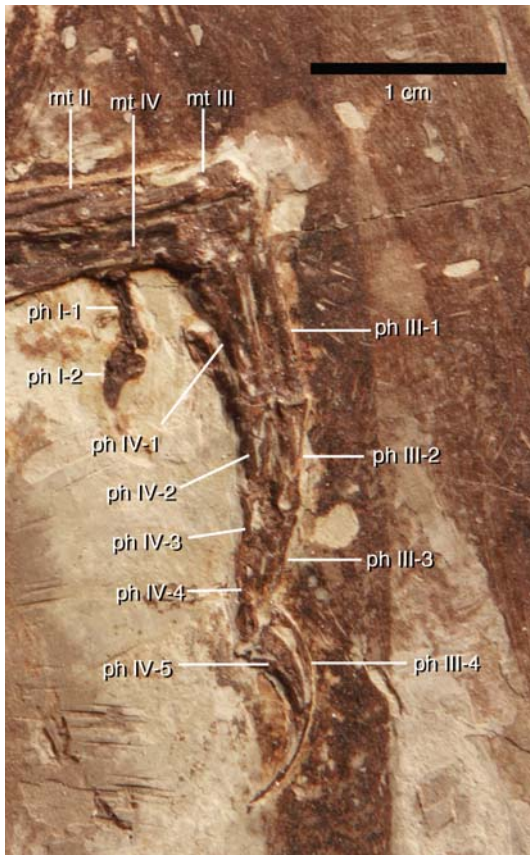


FIGURE 14. The right pedal phalanges of BMNH PH881 in lateral view.

Metatarsal IV is straight, but it is slightly shorter and more robust than metatarsal III. The proximal end of metatarsal IV is square and it is probably fused with the distal tarsals. A prominent ventral ridge is developed along the shaft, which is also observed in the holotype IVPP V12330 (Xu et al., 2000), as a widespread feature of dromaeosaurids. The distal condyles are ventrally placed and distinct ligamental pits are developed on each side. Metatarsal V is slender and bowed. It is attached posterolaterally to metatarsal IV on the proximal end. The distal half of metatarsal V is expanded and flattened, similar to other dromaeosaurids, such as *Sinornithosaurus* (Xu et al., 1999).

In both feet, all the phalanges are well preserved (figs. 14, 15). Digit I, as exposed on both sides of the specimen, is short and slender, and the unguis phalanx I-2 is smaller than other unguis phalanges like in most dromaeosaurids, but not as enlarged as in *Balaur* (Brusatte et al., 2013). The second digit on both sides is obscured by other digits, and thus difficult to observe. Pedal phalanx III-1 is the longest phalanx observed in both feet, while phalanges III-2 and III-3 are subequal in length. Pedal phalanx IV-1 is the longest and phalanx IV-3 is the shortest among all phalanges in digit IV, as described in the holotype IVPP V12330 and the referred specimens CAGS 20-7-004 and CAGS 20-8-001 (Hwang et al., 2002). The unguis phalanx III-4 is slightly

and fibular crest are not prominent. The proximal end of the fibula is expanded, about one third to one fourth of the width of the proximal tibia. Distally, the fibular shaft rapidly thins to a very slender splint that adheres closely to the tibia. The astragalus and the calcaneum appear fused with each other and this compound element is fused with the tibia, as noted in the holotype IVPP V12330 and the referred specimen CAGS 20-8-001 (Xu et al., 2000; Hwang et al., 2002).

A platelike tarsal is visible in this specimen between the left tibiotarsus and the left pes, though the identity of the tarsal is uncertain. However, the distal tarsals are fused to the metatarsals in the referred specimen CAGS 20-8-001 (Hwang et al., 2002).

In BMNH PH881, both feet are exposed in lateral view (figs. 14, 15). Metatarsal IV is well exposed, while metatarsals II and III are partially hidden. Metatarsal III is straight, with a ginglymoid distal end. The distal end of metatarsal III is probably orientated slightly above the plane that metatarsal II and metatarsal IV lie in, evidenced by the slight uplifting of metatarsal III as seen in lateral view.

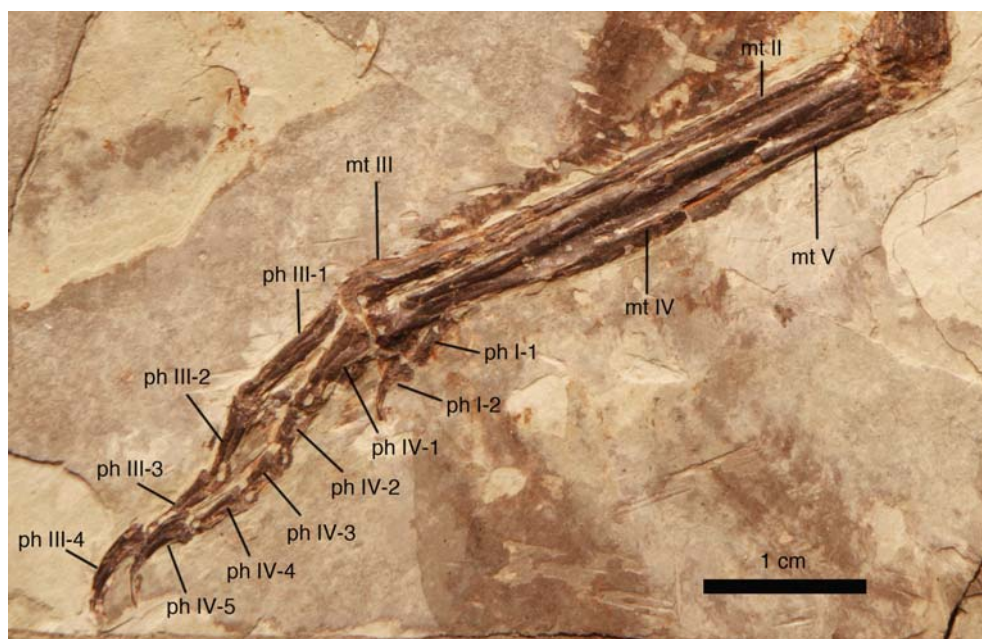


FIGURE 15. The left pes of BMNH PH881 in lateral view.

larger than IV-5, but similar in morphology, with the large flexor tubercles and high degrees of curvature typical of dromaeosaurids (Norell and Makovicky, 2004).

DISCUSSION

As noted by Xu et al. (2002) and amended by Turner et al (2012), several features can be used to refer *Microraptor* to the Dromaeosauridae. These features include the extremely elongate prezygapophyses and chevrons, the retroarticular process of the mandible bearing a distinct vertical process at its posteromedial corner, and a short manual phalanx III-2. This new specimen of *Microraptor* not only confirms these shared derived characters, but also provides new cranial anatomical information supporting this assertion, which is the dorsal displacement of the maxillary fenestra and a large quadrate foramen.

As noted by Xu et al. (2000) and Hwang et al. (2002), *Microraptor* shares several characters with troodontids, including a short subnarial process of the premaxilla, smaller premaxillary teeth than maxillary teeth, the absence of denticles on the anterior carinae of maxillary teeth, and a subarctometatarsalian condition of the pes. BMNH PH881 adds additional characters to this list, such as a shallow main premaxillary body, the relatively large maxillary fenestra and a slender interfenestral bar on the maxilla. These characters, however, have been shown to be present at the more inclusive level of Deinonychosauria in phylogenetic analysis (Turner et al., 2012), and strongly support the sister-group relationship between troodontids and dromaeosaurids; therefore, it is not surprising to find these characters in both troodontids and the basal dromaeosaurid *Microraptor*.

Within dromaeosaurids, *Microraptor* has many similarities with other small dromaeosaurids from the Jehol Biota, such as *Sinornithosaurus* and NGMC 91 (Xu et al., 1999; Ji et al.,

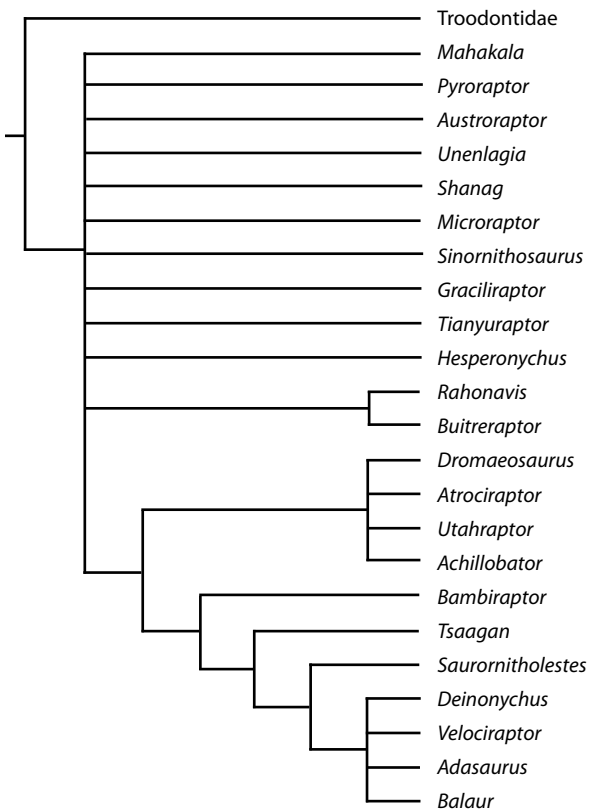


FIGURE 16. Simplified cladogram showing the strict consensus topology of Dromaeosauridae after Turner et al. (2012).

2001). These shared characters include a very short deltopectoral crest on the humerus, the presence of a large supra-coracoid fenestra on the coracoid, and the presence of a lateral tubercle on the midshaft of the pubis. These characters have been proposed as synapomorphies of a monophyletic Jehol dromaeosaurid group (Xu, 2002). *Microraptor*, *Sinornithosaurus*, and NGMC 91 also share a proportionally short manual digit I, which is proposed as a synapomorphy of the Microraptorinae (Senter et al., 2004; Turner et al., 2012). Interestingly, *Sinovenator* and *Jinfengopteryx*, basal troodontids from the Jehol Biota, also have the pubic lateral tubercle present in some specimens, although phylogenetic analysis shows that this feature appears separately in Jehol troodontids and Jehol dromaeosaurids (Turner et al., 2012).

The maxillary fenestra of BMNHC PH881 is unique due to its relatively large size and the presence of an upper fossa and a lower fenestra separated by a

thin bar. This is a condition that has not been reported in any other dromaeosaurids. The maxillary fenestra of *Microraptor* is nearly half the size of the antorbital fenestra, and it is much larger than in other dromaeosaurids where the maxillary fenestra is less than one fourth the size of the antorbital fenestra. The position of the maxillary fenestra in *Microraptor* is relatively dorsal compared with the antorbital fenestra, which is a typical dromaeosaurid condition (Turner et al., 2007b). In contrast, basal troodontids, such as *Sinovenator* and *Anchiornis*, have maxillary fenestrae of comparable size as in *Microraptor*, but are positioned more ventrally (Xu et al., 2002; Hu et al., 2009). The maxillary fenestra of *Microraptor* retains an intermediate state between basal troodontids and many derived dromaeosaurids, which supports the relatively basal phylogenetic position of *Microraptor* in dromaeosaurids and the sister-group relationship between dromaeosaurids and troodontids. Thus, the relatively dorsal position of the maxillary fenestra is a synapomorphy of *Microraptor* and other dromaeosaurids, while the relatively large size of the maxillary fenestra is a plesiomorphy that is retained in primitive deinonychosaurian taxa, such as *Microraptor*, and basal troodontids. Other dromaeosaurids, such as *Shanag*, *Velociraptor*, and *Bambiraptor* bear a maxillary fenestra within a shallow, caudally or caudodorsally open fossa (Turner et al., 2007b). It is possible that the upper fossa of the maxillary fenestra in BMNHC PH881 may in fact represent this caudally open fossa, which is confluent with an

excavatio pneumatica in these dromaeosaurid taxa.

With the new anatomical information of BMNH PH881, we updated the Theropod Working Group (TWiG) matrix by Turner et al. (2012). Eighty characters are updated for *Microraptor*, most of which are from the cranium, and the rest are mainly from the rib cage. Phylogenetic analyses with the updated matrix resulted in similar topologies as the analyses of Turner et al. (2012). The strict consensus topology remains the same, in which many primitive dromaeosaurids including *Microraptor*, *Mahakala*, *Sinornithosaurus*, *Graciliraptor*, *Hesperonychus*, *Tianyuraptor*, *Shanag*, *Buitreraptor*, and the derived dromaeosaurid lineage form a polytomy at the base of Dromaeosauridae (fig. 16). The characters that support the dromaeosaurid node and their polarities are unchanged. By removing *Pyroraptor* from the analysis due to the extremely fragmentary nature of the material (as per Turner et al., 2012), the same reduced strict consensus topology (fig. 17)

is generated. *Microraptor*, *Sinornithosaurus*, *Graciliraptor*, *Tianyuraptor*, and *Hesperonychus* form a group in this reduced topology, and the character set supporting this node is unchanged.

The gastralial and uncinat processes of BMNH PH881 are very well preserved. The presence of gastralial is widely distributed in saurischian dinosaurs (Claessens, 2004). Some information on gastralial has been reported from other small theropods, including dromaeosaurid dinosaurs such as *Sinornithosaurus* and *Velociraptor*, whose middle segments are apparently shorter than lateral segments (Norell and Makovicky, 1997; Xu et al., 1999; Claessens, 2004). BMNH PH881 displays features incongruent with these taxa in having subequal middle and lateral segments, which is more similar to the condition in the volant avialan *Confuciusornis* (Chiappe et al., 1999). Ossified uncinat processes are preserved in some dromaeosaurids and oviraptorosaurs as well as early avialans, such as *Confuciusornis* and *Jixiangornis* (Chiappe et al., 1999; Ji et al., 2002). The morphology of uncinat process of *Microraptor* is very similar to these taxa. Codd et al. (2008) noticed that the uncinat processes of nonavialans are not reduced as in extant cursorial birds, but are of intermediate to long lengths and resemble those of the flying or diving birds. They suggested uncinat processes, in conjunction with lateral and ventral movements of the gastral basket, provide a mechanism for facilitating avianlike breathing mechanics in nonavian maniraptoran dinosaurs. Among nonavian maniraptoran dinosaurs and Mesozoic avialans, the morphology of uncinat process and gastral

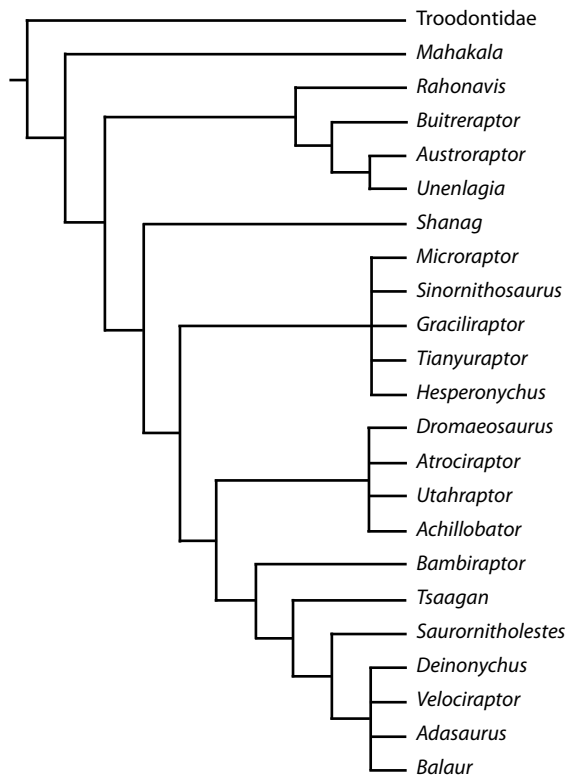


FIGURE 17. Simplified cladogram showing the reduced strict consensus topology of Dromaeosauridae by removing *Pyraptor* after Turner et al. (2012).

TABLE 1. Select Measurements (in mm) of BMNHC PH881.

	Left	Right
Skull length		>48.4
Skull height		21.5
Mandible length	42.5	44.2
Hyoid length		>18.7
Humerus	42.5	47.4
Ulna		44.7
Radius		41.0
Metacarpal I		13.0
Metacarpal II		31.8
Metacarpal III		>29.8
Manual phalanx I-1		12.8
Manual phalanx I-2		11.9
Manual phalanx II-1		13.4
Manual phalanx II-2		12.5
Manual phalanx II-3	>8.1	12.0
Manual phalanx III-1		5.3
Manual phalanx III-2		7.6
Manual phalanx III-3		7.2
Manual phalanx III-4	5.0	5.3
Ilium	>27.8	
Pubis	46.2	
Femur	51.8	52.1
Tibiotarsus	70.7	72.9
Metatarsal II		36.2
Metatarsal III	39.0	38.5
Metatarsal IV	36.1	36.1
Pedal phalanx I-1		4.6
Pedal phalanx I-2		6.0
Pedal phalanx III-1	10.4	8.9
Pedal phalanx III-2	6.4	5.4
Pedal phalanx III-3	6.0	>5.2
Pedal phalanx III-4	10.6	10.5
Pedal phalanx IV-1	7.8	8.2
Pedal phalanx IV-2	4.7	4.8
Pedal phalanx IV-3	4.0	3.8
Pedal phalanx IV-4	4.8	4.4
Pedal phalanx IV-5	8.3	8.6

basket of *Microraptor* resembles *Confuciusornis* most closely. Thus the rib cages of *Microraptor* and the early volant avialans could very likely share a similar mechanism to assist respiration.

Recently, a nominal species *Microraptor hanqingi* was reported based on a single specimen (LVH 0026) from western Liaoning, China (Gong et al., 2012). *Microraptor hanqingi* has been proposed as a new taxon and diagnosed with the following characters: largest known species of *Microraptor*; sternals not fused; robust pubis with square distal end and not bent backward as much as in *M. gui* (IVPP V13352); pubic boot tapering posteriorly; ischia with posterior edge straight and ventral edge concave; a proportionally short manual digit I; metatarsals II and IV about the same length; fewer caudal vertebrae than *M. gui*. We find these characters inadequate as diagnostic features. Both *Microraptor zhaoianus* and *Microraptor hanqingi* have unfused sternals, a posteriorly tapering pubic foot, a proportionally short manual digit I, and metatarsals II and IV of subequal length (Xu, 2002; Hwang et al., 2002; Gong et al., 2012). The large size of LVH 0026 is likely ontogenetic or intraspecific variation, which is also observed in living birds, such as common ravens (Marzluff, 2009). Also, *Microraptor* is known to have considerable intraspecific variation in the number of caudal vertebrae. The differences of the shape of the ischium and the pubis are likely to be preservational or ontogenetic rather than diagnostic of a particular *Microraptor* taxon (Turner et al., 2012). Thus, LVH 0026 lacks solid characters to be distinguished from the other specimens of and, importantly, the holotype of *Microraptor zhaoianus* and we regard *Microraptor hanqingi* as a junior synonym of *Microraptor zhaoianus*.

CONCLUSION

An excellently preserved specimen BMNHC PH881 reveals new morphological information of *Microraptor* regarding the skull, the rib cage, the gastralium, and the humerus. This specimen confirms *Microraptor* as a basal dromaeosaurid dinosaur with features such as a dorsally displaced maxillary fenestra and a large quadrate foramen. Phylogenetic analyses updated with new information corroborate the previously established phylogeny and the monophyly of Dromaeosauridae and Deinonychosauria. The morphology of the rib cage of BMNHC PH881 suggests that *Microraptor* and the early volant avialans such as *Confuciusornis* could very likely share a similar mechanism to assist respiration.

ACKNOWLEDGMENTS

We thank the Beijing Museum of Natural History for access to the *Microraptor* specimen BMNHC PH881. We are grateful to Xu Xing and the Institute for Vertebrate Paleontology and Paleoanthropology for access to other *Microraptor* specimens including the holotype. We also thank: Wang Yu for carefully preparing the specimens, Zeng Zhaohui and Liu Di for arranging the lab in Beijing, Mick Ellison for photographing the specimen and preparing the figures, and Jonah Choiniere for carefully reviewing the manuscript. This project was supported by the Division of Paleontology at the American Museum of Natural History, Columbia University, and the Jurassic Foundation.

REFERENCES

- Balanoff, A.M., and M.A. Norell. 2012. Osteology of *Khaan mckennai* (Oviraptorosauria: Theropoda). Bulletin of the American Museum of Natural History 372: 1–77.
- Barsbold, R., and H. Osmólska. 1999. The skull of *Velociraptor* (Theropoda) from the Late Cretaceous of Mongolia. Acta Palaeontologica Polonica 44 (2): 189–219.
- Bever, G.S., and M.A. Norell. 2009. The perinate skull of *Byronosaurus* (Troodontidae) with observations on the cranial ontogeny of paravian theropods. American Museum Novitates 3657: 1–51.
- Burnham, D.A., et al. 2000. Remarkable new birdlike dinosaur (Theropoda: Maniraptora) from the Upper Cretaceous of Montana. University of Kansas Paleontological Contributions New Series 13: 1–14.
- Brusatte, S.L. et al. 2013. The osteology of *Balaur bondoc*, an island-dwelling dromaeosaurid (Dinosauria: Theropoda) from the Late Cretaceous of Romania. Bulletin of the American Museum of Natural History 374: 1–100.
- Chiappe, L.M., S. A. Ji, Q. Ji, and M.A. Norell. 1999. Anatomy and systematics of the Confuciusornithidae (Theropoda: Aves) from the Late Mesozoic of northeastern China. Bulletin of the American Museum of Natural History 242: 1–89.
- Claessens, L.A.P. 2004. Dinosaur gastralia: origin, morphology and function. Journal of Vertebrate Paleontology 24: 89–106.
- Clark, J.M., M.A. Norell, and L.M. Chiappe. 1999. An oviraptorid skeleton from the Late Cretaceous of Ukhaa Tolgod, Mongolia, preserved in an avianlike brooding position over an oviraptorid nest. American Museum Novitates 3265: 1–36.
- Codd, J.R., P.L. Manning, M.A. Norell, and S.F. Perry. 2008. Avian-like breathing mechanics in maniraptoran dinosaurs. Proceedings of the Royal Society B, Biological Sciences 275: 157–161.
- Colbert, E.H., and D.A. Russell. 1969. The small Cretaceous dinosaur *Dromaeosaurus*. American Museum Novitates 2380: 1–49.
- Currie, P.J. 1995. New information on the anatomy and relationships of *Dromaeosaurus albertensis* (Dinosauria: Theropoda). Journal of Vertebrate Paleontology 15: 576–591.
- Elżanowski, A. 2001. A new genus and species for the largest specimen of *Archaeopteryx*. Acta Paleontologica Polonica 46: 519–532.
- Elżanowski, A., and P. Wellnhofer. 1996. Cranial morphology of *Archaeopteryx*: evidence from the seventh skeleton. Journal of Vertebrate Paleontology 16: 81–94.
- Gauthier, J.A. 1986. Saurischian monophyly and the origin of birds. In K. Padian (editor), The origin of birds and evolution of flight: 1–55. San Francisco: California Academy of Sciences.
- Gong, E.-P., L.D. Marin, D.A. Burnham, A.R. Falk, and L.-H. Hou. 2012. A new species of *Microraptor* from the Jehol Biota of northeastern China. Palaeoworld 21: 81–91.
- Hone, D.W.E., H. Tischlinger, X. Xu, and F.-C. Zhang. 2010. The extent of the preserved feathers on the four-winged dinosaur *Microraptor gui* under ultraviolet light. PLoS One 5: 9223.
- Hu, D.-Y., L.-H. Hou, L. Zhang, and X. Xu. 2009. A pre-*Archaeopteryx* troodontid theropod from China with long feathers on the metatarsal. Nature 461: 640–643.
- Hwang, S.H., M.A. Norell, Q. Ji, and K.-Q. Gao. 2002. New specimens of *Microraptor zhaoianus* (Theropoda: Dromaeosauridae) from northeastern China. American Museum Novitates 3381: 1–44.
- Ji, Q., M.A. Norell, K.-Q. Gao, S.-A. Ji, and D. Ren. 2001. The distribution of integumentary structures in a feathered dinosaur. Nature 410: 1084–1087.
- Ji, Q., S.-A. Ji, and H.-B. Zhang. 2002. A new avialan bird *Jixiangornis orientalis* gen. et sp. nov. from the Lower Cretaceous of western Liaoning, NE China. Journal of Nanjing University (Natural

- Sciences) 38: 723–736.
- Li, Q., et al. 2012. Reconstruction of *Microraptor* and the evolution of iridescent plumage. *Science* 335: 1215–1219.
- Makovicky, P.J., and M.A. Norell. 2004. Troodontidae. In D.B. Weishampel, P. Dodson, and H. Osmólska (editors), *The Dinosauria*: 184–195. Berkeley: University of California Press.
- Marzluff, J.M. 2009. Common raven (*Corvus corax*). In J. del Hoyo, A. Elliott, and D.A. Christie (editors), *Handbook of the birds of the world*. Vol. 14, Bush-shrikes to Old World Sparrows: 638–639. Barcelona: Lynx Edicions.
- Norell, M.A., and P.J. Makovicky. 1997. Important features of the dromaeosaur skeleton: information from a new specimen. *American Museum Novitates* 3215: 1–28.
- Norell, M.A., and P.J. Makovicky. 1999. Important features of the dromaeosaur skeleton II: information from newly collected specimens of *Velociraptor mongoliensis*. *American Museum Novitates* 3282: 1–45.
- Norell, M.A., and P.J. Makovicky. 2004. Dromaeosauridae. In D.B. Weishampel, P. Dodson, and H. Osmólska (editors), *The Dinosauria*: 196–209. Berkeley: University of California Press.
- Norell, M.A., P.J. Makovicky, and J.M. Clark. 2000. A new troodontid theropod from Ukhaa Tolgod Mongolia. *Journal of Vertebrate Paleontology* 20 (1): 7–11.
- Norell, M.A., J.M. Clark, and P.J. Makovicky. 2001. Phylogenetic relationships among coelurosaurian theropods. In J. Gauthier and L.F. Gall (editors), *New perspectives on the origin and early evolution of birds: proceedings of the international symposium in honor of John H. Ostrom*: 49–67. New Haven: Peabody Museum of Natural History.
- Norell, M.A., et al. 2006. A new dromaeosaurid theropod from Ukhaa Tolgod (Ömnögovi, Mongolia). *American Museum Novitates* 3545: 1–51.
- O'Connor, J., Z.-H. Zhou, and X. Xu. 2011. Additional specimen of *Microraptor* provides unique evidence of dinosaurs preying on birds. *Proceedings of the National Academy of Sciences* 108: 19662–19665.
- Ostrom, J.H. 1969. Osteology of *Deinonychus antirrhopus*, an unusual theropod from the Lower Cretaceous of Montana. *Peabody Museum of Natural History Yale University Bulletin* 30: 1–165.
- Russell, D., and Z.-M. Dong. 1993. A nearly complete skeleton of a new troodontid dinosaur from the Early Cretaceous of the Ordos Basin, Inner Mongolia, People's Republic of China. *Canadian Journal of Earth Sciences* 30: 2163–2173.
- Senter, P., R. Barsbold, B.B. Britt, and D.A. Burnham. 2004. Systematics and evolution of Dromaeosauridae (Dinosauria, Theropoda). *Bulletin of the Gunma Museum of Natural History* 8: 1–20.
- Turner, A.H., D. Pol., J.A. Clarke, G. Erickson, and M.A. Norell. 2007a. A basal dromaeosaurid and size evolution preceding avian flight. *Science* 317: 1378–1381.
- Turner, A.H., S.H. Hwang, and M.A. Norell. 2007b. A small derived theropod from Öösh, Early Cretaceous, Baykhangor Mongolia. *American Museum Novitates* 3557: 1–27.
- Turner, A.H., D. Pol., and M.A. Norell. 2011. Anatomy of *Mahakala omnogovae* (Theropoda: Dromaeosauridae), Tögrögiin Shiree, Mongolia. *American Museum Novitates* 3722: 1–66.
- Turner, A.H., P.J. Makovicky, and M.A. Norell. 2012. A review of dromaeosaurid systematics and paravian phylogeny. *Bulletin of the American Museum of Natural History* 371: 1–206.
- Xu, X. 2002. Deinonychosaurian fossils from the Jehol Group of western Liaoning and the coelurosaurian evolution. Ph.D. dissertation, Chinese Academy of Sciences, Beijing, China, 325 pp.
- Xu, X., and X.-C. Wu. 2001. Cranial morphology of *Sinornithosaurus millenii* (Dinosauria: Theropoda: Dromaeosauridae) from the Yixian Formation of Liaoning, China. *Canadian Journal of*

Earth Sciences 38: 1739–1752.

- Xu, X., X.-L. Wang, and X.-C. Wu. 1999. A dromaeosaurid dinosaur with a filamentous integument from the Jiufotang Formation of China. *Nature* 401: 262–266.
- Xu, X., Z.-H. Zhou, and X.-L. Wang. 2000. The smallest known non-avian theropod dinosaur. *Nature* 408: 705–708.
- Xu, X., M.A. Norell, X.-L. Wang, P.J. Makovicky, and X.-C. Wu. 2002. A basal troodontid from the Early Cretaceous of China. *Nature* 415: 780–784.
- Xu, X., et al. 2003. Four-winged dinosaurs from China. *Nature* 421: 335–340.
- Xu, X., et al. 2008. A new feathered maniraptoran dinosaur fossil that fills a morphological gap in avian origin. *Chinese Science Bulletin* 54: 430–435.
- Xu, X., et al. 2010. A new dromaeosaurid (Dinosauria: Theropoda) from the Upper Cretaceous Wulansuhai Formation of Inner Mongolia, China. *Zootaxa* 2403: 1–9.
- Zhang, F.-C., Z.-H. Zhou, X. Xu, X.-L. Wang, and C. Sullivan. 2008. A bizarre Jurassic maniraptoran from China with elongate ribbon-like feathers. *Nature* 455: 1105–1108.

APPENDIX 1

BMNHC PH881 adds new information for the numerical phylogenetic analysis. The data matrix used is from Turner et al.'s (2012) analysis; 80 characters of *Microraptor* are updated.

00??0????????????1000?1?111000?11?2012??01110??0?1???0???????00010100011?1000101
000000??0?1001?1?001?1100?01??0011011212111001?101111110100?11010000110121110101
11023?1?1110211201?11111?000?0001110111110?10000000?11?000??010101111001010?001?
1100?00000?000000?1?10000?000????????????????????0?0?0???000???000000001000?(01)0?00?00
00?001000200???0?000?000??10?0???10100?00000100?0000?0?????000???0?00?00?000000000
0??0?000?00?1000000000??11111110?00?0110?0110110?01?1?1100?1000

APPENDIX 2

ABBREVIATIONS

ac	accessory crest
anp	anterior process of the lacrimal
aof	antorbital fenestra
as	astragalus
c	caudal vertebra
ca	calcaneum
ce	cervical vertebra
dr	dorsal rib
dp	deltpectoral crest
emf	external mandibular fenestra

eco	ectepicondyle
f	femur
fi	fibular
gtr	greater trochanter
h	humerus
hf	humeral foramen
hh	humeral head
hy	hyoid
ifb	interfenestral bar
j	jugal
l	lacrimal
lan	left angular
lar	left articular
lco	lateral condyle
ld	left dentary
lfr	left frontal
li	left ilium
lmf	lower opening of the maxillary fenestra
lms	left medial segment of gastralia
lsp	left splenial
ltr	lesser trochanter
m	maxilla
mc	metacarpal
mco	medial condyle
mf	maxillary fenestra
mt	metatarsal
n	nasal
na	naris
nf	neurovascular foramina
ns	neural spine
op	olecranon process
p	pubis
pa	parietal
pf	pubic foot
pg	popliteal groove
ph	phalanx
pm	premaxilla
pmf	promaxillary fenestra
po	postorbital
poap	postacetabular process of the ilium
pop	posterior process of the lacrimal

poz	postzygapophysis
pra	prearticular
prap	preacetabular process of the ilium
prz	prezygapophysis
ptr	posterior trochanter
q	quadrate
qj	quadratojugal
ra	radius
ran	right angular
rar	right articular
rco	radial condyle
rd	right dentary
rfr	right frontal
ri	right ilium
rls	right lateral segment of gastralia
rms	right medial segment of gastralia
rsp	right splenial
sa	surangular
sc	scapular
se	semilunate
sp	splenial
sq	squamosal
sr	sacral rib
st	sternum
ti	tibia
tu	tubercle of the pubis
u	ulna
uco	ulnar condyle
umf	upper fossa of the maxillary fenestra
up	uncinate process
vp	ventral process of the lacrimal

All issues of *Novitates* and *Bulletin* are available on the web (<http://digitallibrary.amnh.org/dspace>). Order printed copies on the web from:

<http://shop.amnh.org/a701/shop-by-category/books/scientific-publications.html>

or via standard mail from:

American Museum of Natural History—Scientific Publications
Central Park West at 79th Street
New York, NY 10024

Ⓒ This paper meets the requirements of ANSI/NISO Z39.48-1992 (permanence of paper).